32nd EPS Conference on Plasma Phys. Tarragona, 27 June - 1 July 2005 ECA Vol.**29C**, P-1.047 (2005)

Weak Temperature Dependence of the Thermal Diffusivity in High-Collisionality Regimes in LHD

J. Miyazawa[1], H. Yamada[1], S. Murakami[2], H. Funaba[1], S. Inagaki[1], N. Ohyabu[1], A. Komori[1], O. Motojima[1], and LHD experimental group

[1] *National Institute for Fusion Science, Toki, Gifu509-5292, Japan*

[2] *Department of Nuclear Engineering, Kyoto University, Kyoto 606-8501, Japan*

The strong positive dependence on the line-averaged electron density, $\bar{n}_e$, of the energy confinement time, τ_E, as in the international stellarator scaling 1995 (ISS95) [1], where $\tau_E \propto \bar{n}_e^{0.51}$, disappears in the high-density regime in the Large Helical Device (LHD) [2-4]. To investigate the physics behind this, it is important to clarify the parameter dependences of the thermal diffusivity. Here, we define an effective electron thermal diffusivity, χ_e^{eff}, assuming that the density and temperature profiles of ions are equivalent to that of electrons and the heat conductions due to electrons and ions are also the same. When we plot χ_e^{eff} versus the electron temperature, T_e, at least two kinds of temperature dependences seem to appear, *i.e.* one is the gyro-Bohm type ($\chi_e^{eff} \propto T_e^{1.5}$) at the moderate density regime and another is the weak temperature dependence ($\chi_e^{eff} \propto T_e^{0.5}$) at the high-density (and therefore, low-temperature) regime [4]. Other than T_e, χ_e^{eff} also depends on the magnetic field strength, B_0, which denotes the toroidal magnetic field strength on the magnetic axis. Systematic density and power scan experiments have been carried out at various B_0, to precisely investigate the B_0 dependence of χ_e^{eff} in the high-density regime (up to $\langle n_e \rangle \sim 7 \times 10^{19}$ m^{-3}, where $\langle n_e \rangle$ is the volume-averaged electron density). The magnetic configuration is fixed to R_{ax} = 3.6 m, where R_{ax} is the major radius of the magnetic axis in the vacuum configuration. Negative-ion based neutral beam (NB) injection is applied and the total heating power is varied from 2 to 5 MW. The density is scanned by hydrogen gas puffing.

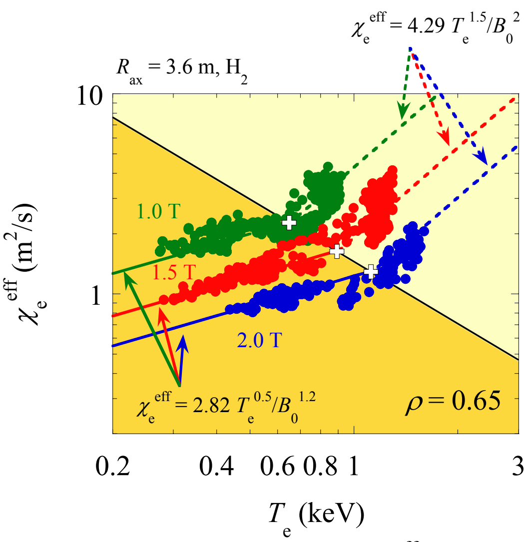

Figure 1. T_e dependence of χ_e^{eff} at various B_0. Solid and broken lines show the best fits for Eqs. (1) and (2). The inflection points are plotted by white crosses.

In Fig. 1, the relations between χ_e^{eff} and T_e at B_0 = 1.0 / 1.5 / 2.0 T are depicted. The weak ($\chi_e^{eff} \propto T_e^{0.5}$) and gyro-Bohm like ($\chi_e^{eff} \propto T_e^{1.5}$) temperature dependences are recognized for each dataset. To estimate the inflection point, T_{e1}, where the temperature dependence of χ_e^{eff} changes from $\chi_e^{eff} \propto T_e^{0.5}$ to $\chi_e^{eff} \propto T_e^{1.5}$, a set of models below is assumed;

$$\chi_e^{eff} = C_1\, T_e^{0.5} / B_0^{\alpha}\ (T_e \le T_{e1}), \qquad (1)$$

$$\chi_e^{eff} = C_2\, T_e^{1.5} / B_0^{2}\ (T_e > T_{e1}). \qquad (2)$$

Below the inflection point, χ_e^{eff} increases with $C_1 T_e^{0.5}$ and decreases with an unknown B_0 dependence of an index α. Note that α = 1.0±0.2 was obtained in the former study [4]. Above the inflection point, we simply assume the gyro-Bohm model with a factor C_2. Three parameters of C_1, C_2 and α are determined at each normalized radius, ρ (= r/a, where a is the averaged minor radius of the last closed flux surface), to give the minimum standard deviation, σ, of the experimental χ_e^{eff} compared with the model. As summarized in Fig. 2, the best solutions of C_1, C_2 and α are obtained at $0.6 \le \rho \le 0.85$, with small standard deviations of less than 2% (Fig. 2 (b)). From Fig. 2 (a), we conclude that α = 1.2±0.1, which is consistent with the former result of α = 1.0±0.2, while the ambiguity is reduced. C_1 is approximately constant (or, it slightly increases with ρ, at $\rho > 0.7$, see Fig. 2 (c)). This is also consistent with the former result. C_2 monotonically increases with ρ (Fig. 2 (d)). The best set of C_1 and C_2 for a fixed α of 1.2, which are depicted by open squares in Fig. 2 (c) and (d), also gives reasonable fittings with small σ (open squares in Fig. 2 (b)) and these are similar to that obtained for the best α. The inflection point is calculated by $T_{e1} = (C_1/C_2)\, B_0^{2-\alpha}$. The radial profile of T_{e1} is a decreasing function of ρ (reflecting the C_2 profile) and increases with $B_0^{0.8\pm0.1}$ (Fig. 2 (e)).

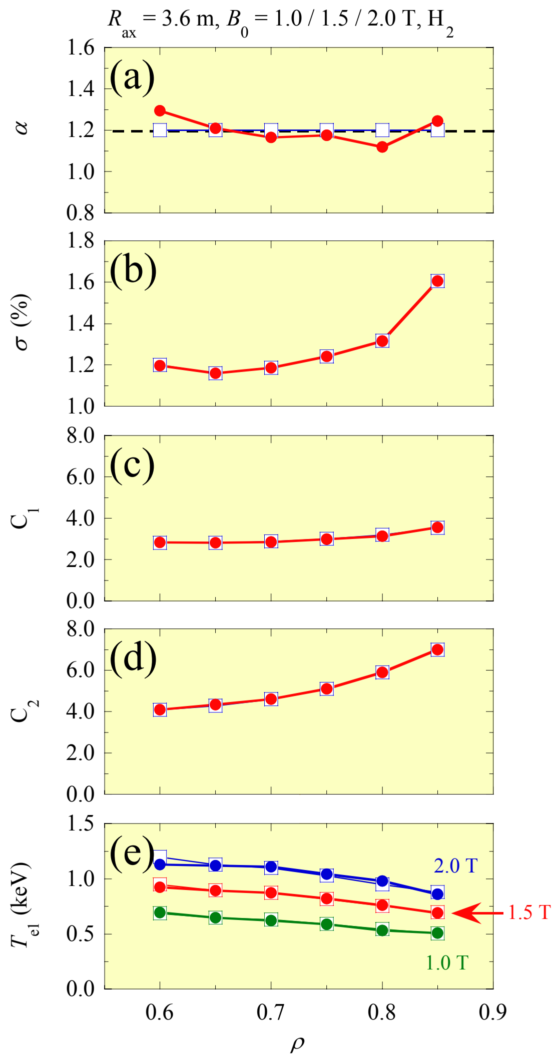

Figure 2. Summary of the fitting results. Closed symbols denote the results with the best α and open symbols denote the results with a fixed α of 1.2.

If the thermal diffusivity can be expressed with experimental parameters, as in Eqs. (1) and (2), it is possible to construct a global confinement scaling. In the former study [4], a global confinement scaling is deduced from the relation of $\chi_e^{eff} \propto T_e^{0.5}/B_0$. Here, we reconsider it by adopting $\chi_e^{eff} \propto T_e^{0.5}/B_0^{1.2}$, which well reproduces χ_e^{eff} in the outer region of $0.6 \leq \rho \leq 0.85$, as long as $T_e \leq T_{e1}$. To obtain a dimensionally correct expression, another dependence on the minor radius of $\chi_e^{eff} \propto a^{-0.5}$ should be introduced as below;

$$\chi_e^{eff} \propto (T_e/a)^{0.5} / B_0^{1.2}. \quad (3)$$

Assuming that $\tau_E^{model} \propto a^2/\chi_e^{eff}$, Eq. (3) is transformed to

$$\tau_E^{model} \propto P_{tot}^{-1/3} <n_e>^{1/3} B_0^{4/5} a^{7/3} R^{1/3}. \quad (4)$$

where P_{tot}, and R denote the total heating power and the plasma major radius, respectively. This can also be expressed by non-dimensional parameters [5], *i.e.*

$$\tau_E^{model} \propto \tau_E^{Bohm} a^0 \rho_*^{-0.8} \nu_*^{-0.3} \beta^{0.3}, \quad (5)$$

where τ_E^{Bohm}, ρ_*, ν_*, and β are the Bohm confinement time, the ion gyro radius normalized by a, the collisionality, and the plasma beta, respectively. Since its non-dimensional form (Eq. (5)) is independent of a, Eq. (4) is dimensionally correct.

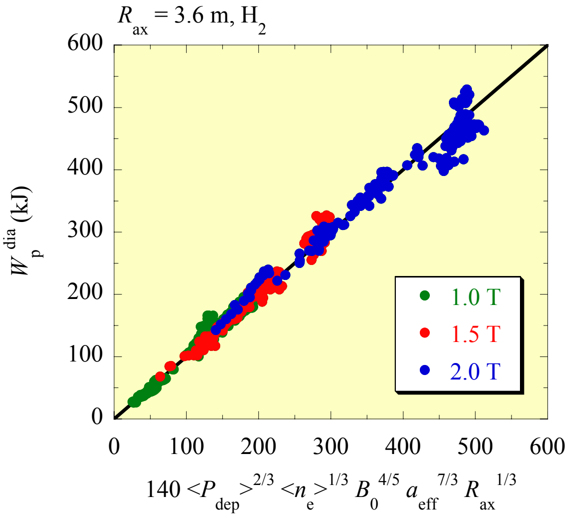

Figure 3. Comparison of the scaling in Eq. (6) with the data from B_0 scan experiment.

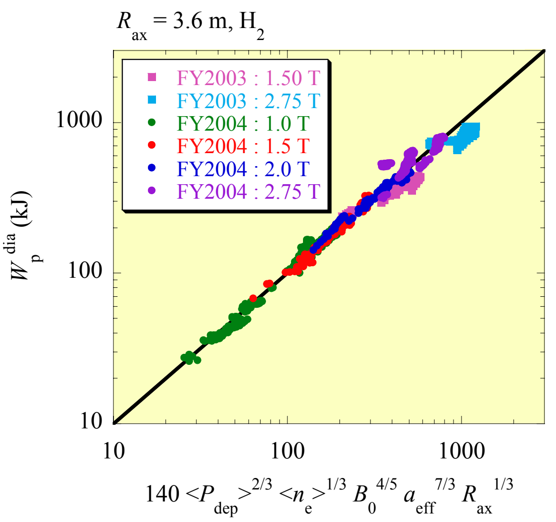

Figure 4. Comparison of the scaling in Eq. (6) with the extended database.

According to Eq. (4), the plasma stored energy should scale as

$$W_p^{HD} \text{ (kJ)} = C <P_{dep}>^{2/3} <n_e>^{1/3} B_0^{4/5} a_{eff}^{7/3} R_{ax}^{1/3}, \quad (6)$$

where units of $<P_{dep}>$, $<n_e>$, and B_0 are MW, 10^{19}m^{-3}, and T, respectively. To include the NB deposition profile effect, which becomes shallower in the high-density regime [2-4], the volume-average of the NB deposition profile, $<P_{dep}>$, is adopted as an index of the heating power. In our case, $<P_{dep}>/P_{tot}$ is ~ 0.8 at $<n_e> < 3\times10^{19}$ m^{-3}, and exponentially decreases with density in the higher density regime ($<P_{dep}>/P_{tot} \sim \exp(-<n_e>/12)$). Here, we define an effective minor radius, a_{eff} (in m), by a product of a and ρ_{100eV}, where ρ_{100eV} is the average ρ where T_e ranges from 50 to 150 eV. This T_e range is chosen because the reliability of our Thomson scattering system is assured at T_e > 30 eV. The effective minor radius is distributed within roughly ±5 % of 0.64 m, which corresponds to a in the vacuum configuration. As for the major radius, we adopt R_{ax} (in m), for simplicity. Due to the Shafranov-shift, the actual R increases to (R_{ax} + 0.1) m in the case of 1 % beta [6], for example. However, this has only negligible impact on the result (less than 1 (3) % for 0.1 (0.3) m of the Shafranov-shift).

The new scaling in Eq. (6) is compared with the datasets of the B_0 scan experiment in Fig. 3. The factor C = 140 is determined by the least square method using this data. Although the data with $T_e > T_{e1}$ in the core region are also included in the figure, all of the data are well reproduced by W_p^{HD}. This indicates the importance of the plasma property in the peripheral region, where T_e is relatively low and scarcely exceeds T_{e1} (note that σ rapidly increases at $\rho >$ 0.8 and it becomes difficult to determine T_{e1}, see Fig. 2 (b)), while the volume is large. In Fig. 4, an extended database is compared with the new scaling, where datasets of hydrogen gas-fueled plasmas obtained in the experimental campaigns in FY2003 (these are also used in Ref. 4) and FY2004 (including the B_0 scan experiment) are shown. Various experimental conditions are included in the database, *i.e.* B_0 = 1.0 / 1.5 / 2.0 / 2.75 T, P_{NB}^{PT} = 0.8 – 11.9 MW, $\langle n_e \rangle$ = (0.2 – 8.2) × 10^{19} m^{-3}. Again, W_p^{dia} is well reproduced by W_p^{HD}.

It has been shown that χ_e^{eff} has a weak temperature dependence as $\chi_e^{eff} \propto (T_e/a)^{0.5} / B_0^{1.2\pm0.1}$, in the outer region of high-density LHD plasmas. The ambiguity in the B_0 dependence is reduced compared with the former study [4]. The inflection point, where the weak temperature dependence changes to the gyro-Bohm type (~ 1.2 keV at ρ = 0.6 and B_0 = 2 T, for example), increases with $B_0^{0.8\pm0.1}$. Based on these observations and assuming a dimensional constraint, a new global confinement scaling that predicts the stored energy of high-density LHD plasmas at given experimental conditions has been obtained (W_p^{HD}, in Eq. (6)). This new scaling matches well with the experiment. Compared with ISS95 ($\tau_E \propto \bar{n}_e^{0.51} P_{tot}^{-0.59}$) [1], our scaling has a weaker density dependence ($\tau_E \propto \langle n_e \rangle^{1/3}$). However, it should be noted that our scaling is still favorable because the density dependence is positive and, especially, the power degradation is weak ($\tau_E \propto \langle P_{dep} \rangle^{-1/3}$).

References

[1] U. Stroth *et al.*, Nucl. Fusion **36**, 1063 (1996).
[2] H. Yamada *et al.*, Nucl. Fusion **43**, 749 (2003).
[3] J. Miyazawa *et al.*, J. Plasma Fusion Res. **81**, 302 (2005).
[4] J. Miyazawa *et al.*, Plasma Phys. Control. Fusion **47**, 801 (2005).
[5] U. Stroth, Plasma Phys. Control. Fusion **40**, 9 (1998).
[6] O. Motojima *et al.*, submitted to Nucl. Fusion.